NANO-RAMAN SPECTROSCOPY: INSTRUMENT DESIGN AND TECHNIQUES

by Kevin C. Hewitt

The ability to obtain information on a nanometer scale is of importance in many fields – spectroscopy being no exception. Raman spectroscopy is the inelastic scattering of light. Light is preferentially scattered at wavelengths that depend on the structure and environment of the material under study. In fact, these set of wavelengths in the Raman spectra is a unique fingerprint of the material. To obtain this information on a nanometer scale would enable many advances that include biophysics applications such as the ability to distinguish healthy and diseased tissue at the nanometer scale, and condensed matter physics studies of nano-sized objects such as quantum dots.

The major issue in the collection of spectra from such small volumes is the signal-to-noise ratio. I will review the variety of techniques and instrument designs employed to enhance the signal. In particular, nano-Raman spectroscopy is reviewed in the context of both near-field and surface enhanced Raman spectroscopy.

The ability to obtain information on a nanometer scale is of importance in many fields – spectroscopy being no exception. I will review nano-Raman spectroscopy in the context of both near field and surface enhanced Raman spectroscopy.

INTRODUCTION

Raman spectroscopy is the inelastic scattering of light. In particular, one illuminates the sample of interest with laser light. Most of the light is scattered elastically at the same wavelength, and this process is referred to as Rayleigh scattering. Weaker components of light scattered at different wavelengths are a signature of the sample under study. These set of wavelengths are characteristic of the chemical bonding in the material. It is these latter inelastically scattered components that are of interest in a Raman scattering experiment. Nano-Raman spectroscopy, therefore, represents one of the few techniques that yield chemical information on the nanoscale without damaging the samples. When used in conjunction with an Atomic Force Microscope (AFM), it can also provide a topographic image to correlate with the Raman spectra. The weakness of the light intensity of these features is one of the main reasons that nano-Raman spectroscopy has not found wider applicability to date. The cross section for Raman scattering ($\sim 10^{-30}$ cm^2) is much lower than infrared absorption ($\sim 10^{-20}$ cm^2) or fluorescence ($\sim 10^{-16}$ cm^2).

In a conventional Raman spectroscopy experiment using a microscope, there exists a diffraction limited resolution on the order of the wavelength of light. In order to obtain spectral information with a much smaller spatial resolution researchers turned to near-field optical microscopy, establishing the field of nano-Raman spectroscopy. In 1995, Catherine Jahncke, Michael Paesler and Hans Hallen were the first to combine Raman spectroscopy with near-field scanning optical microscopy [1]. While these pioneers used a subwavelength aperture to illuminate the sample in the near-field, Anderson [2], Hayazawa *et al.* [3] and Stöckle *et al.* [4] were the first, in 2000, to use the metallized tip of an AFM to produce nano-Raman images. The former technique has been given the name apertured and the latter apertureless nano-Raman spectroscopy. These techniques have been reviewed recently by Hallen and Jahncke [5] for this 10-year old field.

NanoRaman spectroscopy has not been used more broadly because, as discussed above, the signals are very small. In apertured nano-Raman spectroscopy the illumination levels at the sample are in the tens of nanowatts and the scattering cross sections are very small, so one obtains very low signal levels. However, apertureless nano-Raman spectroscopy, by virtue of the fact that it uses nanoscale metallic structures (i.e. the AFM tip), offers field enhancement of several orders of magnitude. The most spectacular demonstration of the effect of this enhancement was the recent report of high resolution near-field Raman imaging of single walled carbon nanotubes by Achim Hartschuh and Lucas Novotny at the Institute of Optics, Rochester, Erik Sanchez at Portland State and X. Sunney Xie at Harvard University [6]. They imaged carbon nanotubes with a spatial resolution of ~ 25 nm, owing to a field enhancement of 10^3. Instrument manufacturers such as Jobin-Yvon are developing prototypes for the commercial markets, while Renishaw and WiTec have already entered the market with, respectively, their Nanonics NSOM/SPM™ and AlphaSNOM™ probe.

The review proceeds as follows. Section II outlines near-field scanning optical microscopy (NSOM). Section III discusses the details of apertured vs apertureless nano-Raman spectroscopy. The localized fields that are particular to near-field techniques have led to the development of altered selection

PACS numbers: 07.60.-j,39.30.+w,78.30.-j,78.20.-e,63.20.-e, 63.22.+m.

Kevin C. Hewitt <Kevin.Hewitt@Dal.ca>, Dalhousie University, Department of Physics and Atmospheric Science, Halifax, NS, B3H 3J5

rules as described by Gradient field Raman (GFR) spectroscopy (Section IV). The review ends with a short summary in section V.

NEAR-FIELD SCANNING OPTICAL MICROSCOPY (NSOM)

In Raman scattering experiments, diffraction effects normally limit the spot size of the incident light, of wavelength λ, on the sample to $s = 2.44f\lambda/D$, for a lens of focal length f and limiting aperture diameter D. The irradiance is a diffraction pattern with most of the light collected in a central Airy disc. One can express this limit in terms of the numerical aperture (N.A. = nsinα) of a lens, which defines the cone of rays whose maximal half-angle, α, are accepted by the lens when it is immersed in a medium of index of refraction n. The diffraction limited spot size, or the diameter of the disc for which the objective lens of a microscope accepts light, is $s = 1.22\lambda/\text{N.A.}$ The 100× objective lens of a microscope in air (n=1) has a N.A. of about 1, leading to a minimum spot size of λ. As such, incident light with a wavelength of 500 nm produces a diffraction limited spot size of approximately 0.5 micron using the 100× objective lens of a microscope. By using an oil immersion lens whose numerical aperture can be 1.4, the diffraction limited spot for a 500 nm laser can be no less than 435 nm.

The Airy disc is a consequence of far-field, or Fraunhofer, diffraction from a subwavelength aperture. This limitation is removed by working in the near field, or Fresnel, limit. The boundary between these limits- is governed by the distance, l, of the source or observation point relative to the size of the aperture (e.g. lens) and the wavelength. If the aperture has an area A and the wavelength is λ, the near-field limit is valid for $l < A/\lambda$, (see, for example, Pedrotti and Pedrotti [7]). Assuming visible light with a nominal wavelength of 500 nm incident on a subwavelength circular aperture ($A=\pi r^2 = \frac{1}{4}\pi d^2$) of diameter $d = \lambda/m$ ($m > 1$), the aperture must be placed at a distance from the sample no more than $\lambda/(4m^2)$. If the aperture is 1/5 the wavelength (m=5), then the aperture-sample distance can be no more than 16 nm. Distance control to this degree can only be obtained by using an atomic force microscope. By ensuring that the sample or observation point is placed at this distance one can obtain spatial information with a resolution equal to the size of the aperture. This configuration, termed near-field, allows one to obtain submicron information.

Therefore, in order to obtain near-field spectra one must have:

- a subwavelength aperture or conjugate aperture (i.e. a point).
- the ability to position the aperture in the near field - e.g. at a distance ~ 10 nm from a sample of interest
- instrument stability

In general terms, the near-field limit is valid in situations where either or both source and observing screen are close enough to the aperture that wavefront curvature must be taken into account. The far-field portion, the planar wavefronts, propagate away from the wavefront and can be focused by conventional lenses while the near-field portion remains localized around the aperture in a region less than a wavelength in size.

APERTURED VS APERTURELESS NANO-RAMAN SPECTROSCOPY

Initial attempts by Pohl *et al.* [8] in 1984 to obtain NSOM (not Raman) images used optical fibers which were coated with aluminum except for a small aperture at the end of the fiber - apertured NSOM. In 1994, Zenhausern *et al.* [9] used the tip of an AFM probe, which can be coated with a metal such as gold or silver - apertureless NSOM. In both cases the dimensions of the aperture or tip are in the range of tens to hundreds of nanometers, i.e. subwavelength sizes. These two general techniques were applied to Near-field Raman spectroscopy, i.e. Nano-Raman spectroscopy and are described below.

Configurations

Two scattering modes must be defined in order to make sense of the discussion. Near- field spectroscopy is possible if either the source or collection optics is in the near field of the sample. Thus one can define two configurations, collection or illumination mode. As one can guess from the terms, **illumination mode** describes a configuration in which the source is the near-field and the collection optics is in the far field. Conversely, in **collection mode** the collection optics is in the near field and the source in the far field.

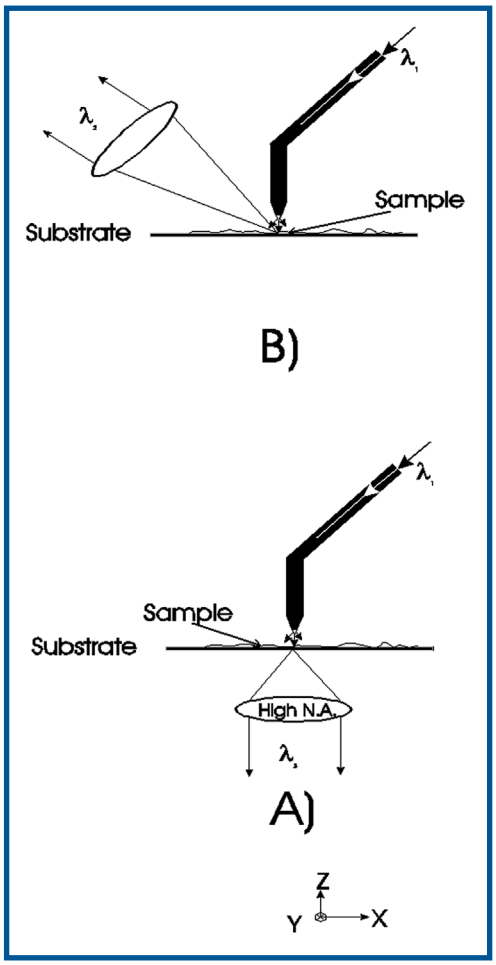

Fig. 1 **Illumination mode apertured NSOM in (a) transmission and (b) reflection. Input laser, λ_1, and scattered light collected by Raman spectrometer denoted λ_2.**

While one may illuminate the sample or collect scattered light in the near field for apertured nano-Raman spectroscopy, the same is not true for apertureless nano-Raman spectroscopy. In the latter case, the tip acts solely as a source of evanescent waves in the near field and collection can be made in the far field.

One can also arrange the optics in reflection or transmission for both apertured and aperturless nano-Raman spectroscopy. These options are summarized in Figs. 1 and 2 for illumination mode and collection mode apertured nano-Raman spectroscopy, respectively. All the reports in the literature use transmission geometry for aperturless Raman spectroscopy (Fig. 3), although it is possible to use reflection geometry.

Apertured - Long collection times (e.g. 10 hrs)

NSOM was first proposed by Synge [10] in 1928 and demonstrated by Ash and Nicholls [11] at microwave frequencies (corresponding to λ = 3 cm) with a resolution of ~ $\lambda/60$. NSOM at optical frequencies (λ = 514.5 nm) using a fiber probe was first reported by Betzig [12] in 1991 with a resolution of $\lambda/43$. Jahncke, Paesler and Hallen [1,13] were the first to combine NSOM with Raman spectroscopy. They used illumination mode in transmission geometry to image Rb-doped $KTiOPO_4$. A far field objective collected light scattered from an NSOM fiber tip. Emphasis was placed on having a stable instrument because of the weak Raman signals (see Fig. 4). In fact, the system had to be stable for a period of at least ten hours as one needed to have at least that length of time to collect a reasonable spectral image from a 4 μm^2 area! These long collection times were the main reason the technique did not find wide applicability.

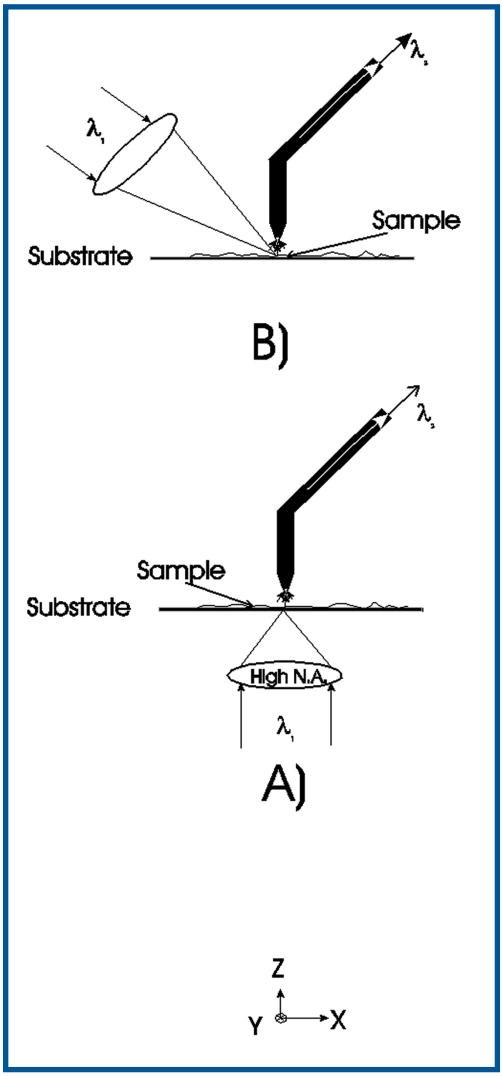

Fig. 2 Collection mode apertured NSOM in (a) transmission and (b) reflection. Input laser, λ_1, and scattered light collected by Raman spectrometer denoted λ_2.

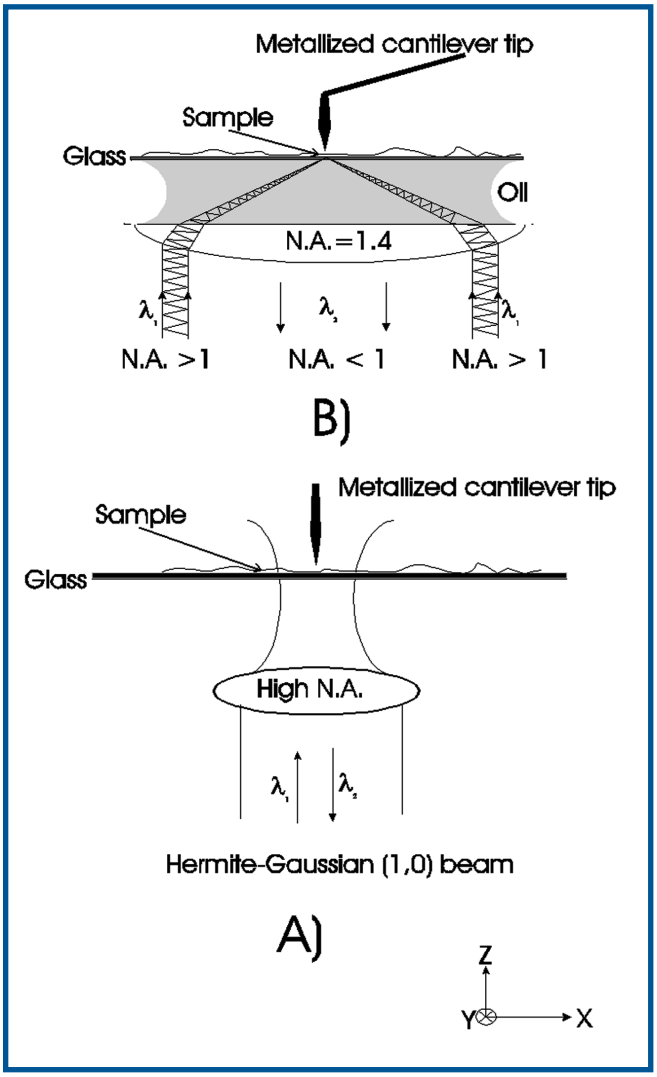

Fig. 3 Apertureless NSOM producing exciting radiation along the tip axis (z) using (a) evanescent waves produced by total internal reflection or (b) (0,1) Hermite Gaussian mode. Input laser, λ_1, and scattered light collected by Raman spectrometer denoted λ_2.

Apertureless - Short collection times (e.g. 10 mins)

In 1989, Wickramassinghe and Williams were the first to propose [14] and then demonstrate [9] the idea of using spherical light scattering from the tip of a standard Atomic Force microscope (AFM) or scanning tunneling microscope (STM) to define the light source, rather than transmitting light through a fine aperture. Stöckle, Suh, Deckert and Senobi [4] were the first (Feb. 2000) to demonstrate its use in Raman spectroscopy. Novotny, Xie and co-workers carried out extensive development of the theory of scattering by metal tips [15–18] and have recently produced high resolution Raman images of carbon nanotubes that clearly demonstrate the feasibility of the technique (Fig. 5).

It has been found [15] that electric field enhancement (see section on Electric Field Enhancement) is possible only if the polarization is parallel to the axis of the tip (i.e. z-axis in Fig. 3). To obtain light polarized along the axis of the tip, two methods have been employed - an evanescent field [3] or higher order Hermite Gaussian mode [16].

Hayazawa *et al.* [3] inserted a circular mask in the beam path of the illumination light, located at the conjugate plane of the pupil of the objective lens which had a numerical aperture of 1.4. The mask rejects the part of the beam corresponding to focusing angles that are less than N.A. = 1, while the transmitted light forms a focused spot that produces an evanescent field on the sample surface. The highly p-polarized evanescent field excites surface plasmon polaritons at the AFM tip apex.

When the wave penetrates the rare medium by an amount

$$y = \frac{\lambda}{2\pi\sqrt{\frac{\sin^2\theta}{n^2} - 1}}$$

(see. e.g., pg. 420 in Pedrotti and Pedrotti for the derivation [7]), the amplitude is decreased by a factor of 1/e. The energy of this evanescent wave returns to the original medi-

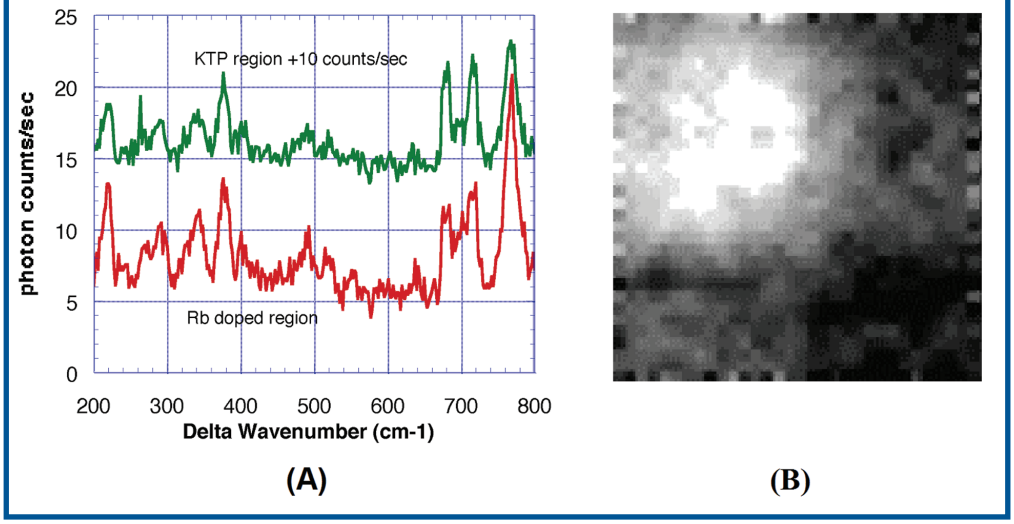

Fig. 4 **(a) Apertured nano-Raman spectra of undoped and Rb-doped $KTiOPO_4$ and (b) the corresponding Raman image [reproduced with permission from Hans Hallen, North Carolina State University, Raleigh, NC, USA].**

um unless a second medium is introduced into its region of penetration. For light of wavelength 514.5 nm undergoing total internal reflection (TIR) at a glass-air interface the penetration depth is about 100 nm - an order of magnitude larger than the tip-sample separation. The evanescent wave moves in a direction along the surface between the two media. That is, its direction of propagation gives rise to the desired electric field properties - polarization parallel to the tip axis.

One may also [16] illuminate using the Hermite Gaussian mode (1,0) and position the tip off the central axis of the focus of the beam to obtain light polarized parallel to the tip axis.

Enhancement

Electric Field Enhancement

By using a metal tip of sub-100 nm scale, one is effectively conducting a Surface Enhanced Raman Scattering (SERS) experiment [19,20]. SERS can increase the intensity of the Raman scattered signal by several orders of magnitude with the introduction of metal particles (or curved surfaces) which have dimensions (a) much less than that of the wavelength (λ) of the incident laser light. SERS relies on the fact that the metal particle contains conduction electrons whose motion is affected by the electric field of the incoming light. If the metal has a high electrical conductivity at the chosen optical frequency, the incident electric field couples to the conduction electrons, causing them to vibrate, and create a dipolar surface plasmon (DSP). Accelerating charges produce electromagnetic radiation so the electrons, in turn, produce radiation at the same frequency as the incident light. However, the amplitude of the secondary radiation may be enhanced, depending on the optical conductivity of the metal, the size and shape of the particle. The enhancement is maximized at a particular wavelength (λ_L) for which the imaginary part of the metal dielectric constant, $\varepsilon_i(\lambda_L)$, is related to that of the real part of the dielectric constant, ε_o of the surrounding medium, by $\varepsilon_i(\lambda_L) = -2\varepsilon_o(\lambda_L)$ [21,22]. The Raman signal is then enhanced because of the increased amplitude of the secondary light.

There is a spatial dependence of the secondary radiation that allows one to tailor the enhancement to a region surrounding the metal particle. For a perfectly spherical particle, theory predicts [23] that the secondary field, and in turn the enhancement, should fall off as $(a/r)^3$ for a particle of size a at a distance r from the centre of the particle. The spatial and excitation wavelength dependence is modified for particles of different shapes as described by Zeman and Schatz [23].

The sensitivity of SERS techniques allows one to detect spectra of dilute species. For example, it has been shown [24] that one monolayer of pyridine can be detected on a roughened silver surface due to a SERS enhancement of 4×10^5 of the 1008 cm^{-1} band. Xu *et al.* [25] recently demonstrated the detec-

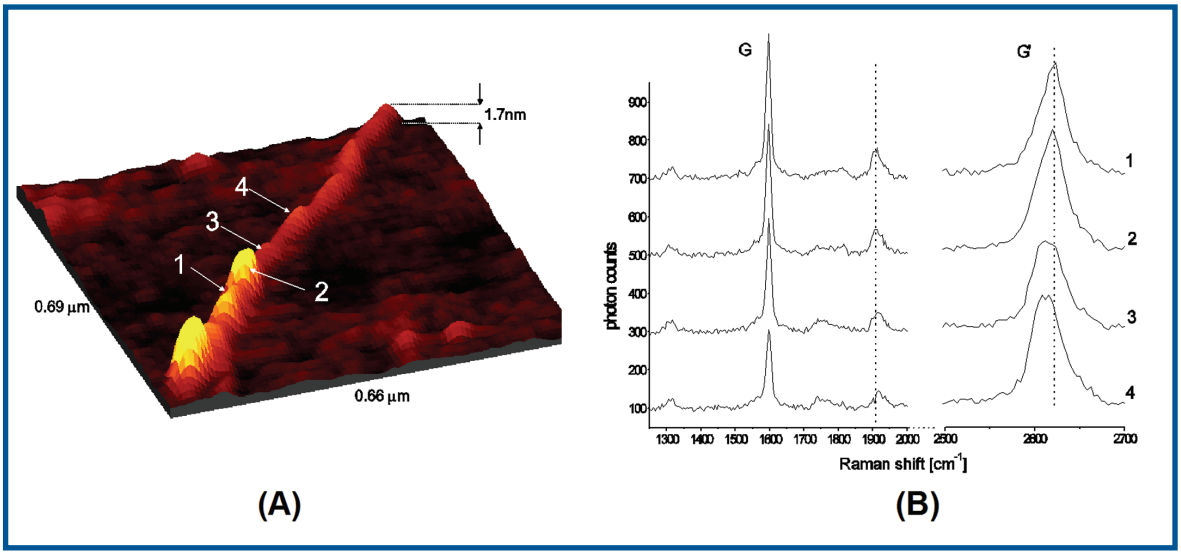

Fig. 5 **(a) High resolution AFM topographic image of a single-walled carbon nanotube, and corresponding (b) apertureless nano-Raman spectra at points indicated in the topographic image showing the tangential stretching mode at 1596 cm^{-1} (G band) and disorder induced overtone mode at 2615 cm^{-1} (G′ band) of carbon [reproduced with permission from Lukas Novotny, University of Rochester, Institute of Optics, Rochester, NY, USA].**

tion of molecular vibrations in single hemoglobin protein molecules (whose size is approx. 5 nm) attached to isolated and immobilized 100 nm silver particles using SERS. In addition, immense enhancement factors of 10^{14} to 10^{15} were obtained by Nie and Emory [26] in the detection of single rhodamine 6G molecules adsorbed on 110-120 nm silver particles using 514.5 nm line, and by Kniepp *et al.* in the detection of a single crystal violet molecule [27] and the single DNA base molecule adenine using 830 nm laser excitation [28].

SERS Active Substrate

Apertureless nano-Raman is effectively a SERS experiment because of the presence of a nanoscale metal tip. To take further advantage of the SERS effect in NSOM applications one may prepare the surface onto which the samples of interest are deposited. The surface can be prepared by depositing nano-sized spheres onto an atomically flat surface such as mica. The spheres are then coated with the metal of interest [29,30], creating a SERS active substrate. Consequently, near field illumination of the sample produces an enhancement due to both the tip and the surface in apertureless nano-Raman. Conversely, apertured nano-Raman will only have a SERS contribution from the active substrate.

Polarization effects

The electric field surrounding the tip or aperture is governed by boundary conditions at the surface of a conductor (see for example Chapter 8 in Jackson [31], esp Fig. 8.1, 8.2). Outside the surface of a perfect conductor only normal electric fields can exist, tangential fields must be zero. The normal and tangential fields are zero inside. In the case of a good, but not perfect, conductor the fields are attenuated exponentially in a characteristic length scale, the skin depth. Thus in the latter case, there is a small tangential electric field, in addition to the normal E field outside the tip.

Given the polarization effects outlined above, one expects more drastic changes in the selection rules between micro- and nano-Raman spectroscopy. The fields in the vicinity of a metallic aperture have components that are predominantly in-plane with a weak contribution out of plane (Bethe-Bouwcamp) [32]. For example, if the field incident through the fiber is polarized in the x-dir'n, there will be weak y- and z-components present near the boundary of the aperture [5]. Thus the sample will be exposed to light of all polarizations, and the spectra will contain all possible modes. Very close to the sample, all components of the electric fields are enhanced under the metallic aperture. As the tip is drawn away from the sample surface, the modes due to y- and z-polarizations will weaken.

In the case of apertureless nano-Raman spectroscopy, the field directly below the tip is oriented parallel to the tip axis (z-axis) [18]. Thus, the sample will be exposed to light polarized perpendicular to the substrate. Therefore, the probe will scatter modes excited by light polarized in the z-direction.

Tip and aperture preparation

Metallic Tip

Tips are prepared by coating AFM tips with a noble metal using physical vapor deposition techniques. Gold and silver coatings have been used with great success. After deposition, the coating can be etched and/or milled using a focused ion beam. Sizes of the order of 10 nm are possible [6].

Metal coated Aperture Tip of a Fiber

To produce fibers which are transmitting, except for an aperture, aluminum is the material of choice for metallization due to its small penetration depth for visible light (~10nm). Transmission coefficients along the fiber core are found to be < 1 % from input to output [33]. The tip is almost completely coated with thin aluminum layer to prevent light leakage when it becomes to narrow for guiding an optical mode. Only at the very end of the tip is there a small aperture where light can emerge.

Heating effects

Fiber Tips

Fibers have a characteristic maximum input power density that is due to the coating material and thickness. Coupling 10 mW into the fibers leads to an increase in the temperature of the tip to 480ºC [34]. The temperature scales linearly with the input light intensity. One must therefore be very careful with the input power. Routine SNOM requires input powers of a few hundred microwatts, leading to an output in the nanowatt regime (measured in the far field) and to tip temperatures well below 50ºC [35]. The ultimate input power limit is determined by these temperature considerations. Damage occurs near 470ºC [34] where Al flakes off due to the difference in thermal expansion co-efficients of the fiber ($4\text{-}9 \times 10^{-6}$ K^{-1}) and aluminum (25×10^{-6} K^{-1}). Deposition of a thicker layer of aluminum and an increased cone angle result in lower temperatures and heating rates [34].

Metal Tip

For apertureless nano-Raman spectroscopy, the temperature of the tip increases due to power dissipation in the skin depth of the surface. For an incident power density of 65 mW/μm^2, the corresponding temperature rise at the surface of the tip is only 6.5 K [15]. Thus experiments can be conducted at an incident power that is larger than that used in apertured nano-Raman spectroscopy.

Spatial resolution

The spatial resolution is governed by the size of the probe, its shape and the distance from the probe to the sample. For both apertured and apertureless configurations, the latter distance can be altered to a similar degree. However, the size of the probe is governed by the limits of the various fabrication techniques that are used in each case. First, the tip of an AFM can be etched and then milled using a focused ion beam, producing tips of 10-15 nm [6] in size. Secondly, fiber apertures are produced by etching the optical fiber and then coating with a metal. Apertures produced in this manner have a realistic lower limit of approximately 20 nm. Therefore, it is evident that the aperturless probe has a spatial resolution that can be two times smaller than apertured probed.

GRADIENT FIELD RAMAN (GFR) SPECTROSCOPY

In the near field limit the electric fields have significant curvature and decay over nanometer length scales. Atoms in the

sample therefore experience a gradient in the electric field that leads to profound changes in the selection rules [36]. Normally, selection rules in micro- or macro-Raman spectroscopy derive from the long wavelength of the incident light relative to the interatomic spacing. In the theoretical expansion of the terms describing the dipole moment, the Raman term depends on the derivative of the product of the polarizability tensor and the electric field with respect to the co-ordinate of vibration, Q. Normally, the electric field is Q independent and one can remove it from the expansion. However, in nano-Raman spectroscopy both are varying, hence an additional term - the product of the polarizabity and the Q-derivative of the electric field - is introduced. This term introduces additional selection rules that lead to the appearance of modes that are normally IR active, Raman inactive, in nano-Raman spectra. Therefore, in addition to the polarization effects outlined in section III C, this GFR effect also alters the number of modes observed in the spectra.

SUMMARY

The field of Nano-Raman spectroscopy is only 10 years old. The recent (2003) experiments using apertureless techniques [6] have highlighted its power in combining the Atomic Force microscope with spectroscopy. Spectra collection times are now reduced to reasonable periods of a few minutes. Apertureless nano-Raman spectroscopy is also effectively a controlled SERS experiment.

Given the application of SERS to problems in materials science, physics, chemistry and biology, it is only a matter of time before apertureless nano-Raman spectroscopy is also applied to these areas.

REFERENCES

1. L. Jahncke, M.A. Paesler, and H.D. Hallen, "Raman imaging with near-field scanning optical microscopy", *Appl. Phys. Lett.* **67**, 2483–2485 (1995).
2. M.S. Anderson, "Locally enhanced Raman spectroscopy with an atomic force microscope", *Appl. Phys. Lett.*, **76**, 3130–3132 (2000).
3. N. Hayazawa, Y. Inouye, Z. Sekkat, and S. Kawata, "Metallized tip amplification of near-field Raman scattering", *Optics Comm.*, **183**, 333–336 (2000).
4. R.M. Stockle, Y.D. Suh, V. Deckert, and R. Zenobi, "Nanoscale chemical analysis by tip-enhanced Raman spectroscopy", *Chem. Phys. Lett.*, **318**,131–136 (2000).
5. H.D. Hallen and C.L. Jahncke, "The electric field at the apex of a near-field probe: Implications for nano-Raman spectroscopy", *J. Raman Spec.*, **34**, 655–662 (2003).
6. A. Hartschuh, E.J. Sanchez, X.S. Xie, and L. Novotny, "High-resolution near-field Raman microscopy of single-walled carbon nanotubes", *Phys. Rev. Lett.*, **90**, 095503–1–4 (2003).
7. F.L. Pedrotti and L.S. Pedrotti, *Introduction to Optics*, Prentice Hall, Upper Saddle River, New Jersey 07458, second edition (1993).
8. D.W. Pohl, W. Denk, and M. Lanz, "Optical stethoccopy: Image recording with resolution λ/20", *Appl. Phys. Lett.*, **44**, 651–653 (1984).
9. F. Zenhausen, M.P. Boyle, and H.K. Wickramasinghe, "Apertureless near-field optical microscope", *Appl. Phys. Lett.*, **65**, 1623–1625 (1994).
10. E. H. Synge, *Phil. Mag.*, **6**, 356 (1928).
11. E.A. Ash and G. Nicholls, *Nature,* **237**, 510 (1972).
12. E. Betzig, J.K. Trautman, T.D. Harris, J.S. Weiner, and R.L. Kostelak, "Breaking the diffraction barrier: Optical microscopy on a nanometric scale", *Science,* **251**,1468–1470 (1991).
13. C.L. Jahncke, H.D. Hallen, and M.A. Paesler, "Nano-Raman spectroscopy and imaging with a near-field scanning optical microscope", *J. Raman Spec.*, **27**:579–586 (1996).
14. H.K. Wickramasinghe and C.C. Williams, "Apertureless near field optical microscope", U.S. Patent 4,947,034, April 28 (1989).
15. L. Novotny, R.X. Bian, and X.S. Xie, "Theory of nanometric optical tweezers", *Phys. Rev. Lett.*, **79**, 645–648 (1997).
16. L. Novotny, E.J. Sanchez, and X.S. Xie, "Near-field optical imaging using metal tips illuminated by higher order Hermite-Gaussian beams", *Ultramicroscopy,* **71**, 21–29 (1998).
17. E.J. Sanchez, L. Novotny, and X.S. Xie, "Near-field fluorescence microscopy based on two-photon excitation with metal tips", *Phys. Rev. Lett.*, **82**, 4014–4017 (1999).
18. A. Bouhelier, M. Beversluis, A. Hartschuh, and L. Novotny, "Near-field second-harmonic generation induced by local field enhancement", *Phys. Rev. Lett.*, **90**, 013903–1–4 (2003).
19. M. Moskovits, "Surface-enhanced spectroscopy", *Rev. Mod. Phys.*, **57**, 783–826 (1985).
20. R.K. Chang and T.E. Furtak, editors, *Surface Enhanced Raman Scattering,* Plenum Press, 233 Spring Street, New York, NY 10013 (1982).
21. R.L. Birke and J.R. Lombardi, *Spectroelectrochemistry Theory and Practice*, pages 263–328, Plenum Press (1988).
22. P.B. Johnson and R.W. Christy, "Optical constants of the noble metals", *Phys. Rev.*, **B 6**, 4370–4379 (1972).
23. E.J. Zeman and G.C. Schatz, "An accurate electromagnetic theory study of surface enhancement factors for Ag, Au, Cu, Li, Na, Al, Ga, In, Zn, and Cd., *J. Phys. Chem.*, **91**, 634–643 (1987).
24. R.P. Van Duyne, *Chemical and Biochemical applications of lasers, volume IV,* Academic Press, New York, NY (1979).
25. H. Xu, E.J. Bjerneld, M. Käll, and L. Börjesson, "Spectroscopy of single hemoglobin molecules by surface enhanced Raman scattering", *Phys. Rev. Lett.*, **83**, 4357–4360, (1999).
26. S. Nie and S. R. Emory, "Probing single molecule and single nanoparticles by surface enhanced Raman scattering", *Science,* **275**, 1102–1106 (1997).
27. K. Kneipp, Y. Wang, H. Kneipp, L.T. Perelman, I. Itzkan, R.R. Dasari, and M.S. Feld, "Single molecule detection using surface-enhanced Raman scattering", *Phys. Rev. Lett.*, **78**, 1667–1670 (1997).
28. K. Kneipp, H. Kneipp, V.B. Kartha, R. Manoharan, G. Deinum, I. Itzkan, R.R. Dasari, and M.S. Feld, "Detection and identification of a single DNA base molecule using surface-enhanced Raman scattering (SERS)", *Phys. Rev.* **E 57**, R6281–R6284 (1998).
29. D. Zeisel, V. Deckert, R. Zenobi, and T. Vo-Dinh, "Near-field surface-enhanced Raman spectroscopy of dye molecules adsorbed on silver island films", *Chem. Phys. Lett.*, **283**, 381–385 (1998).
30. V. Deckert, D. Zeisel, R. Zenobi, and T. Vo-Dinh, "Near-field surface-enhanced Raman imaging of dye-labeled DNA with 100-nm resolution", *Anal. Chem.*, **70**, 2646–2650 (1998).
31. J.D. Jackson, *Classical Electrodynamics*, Wiley, New York, NY, 2nd edition (1975).
32. H.A. Bethe, "Theory of diffraction by small holes", *Phys. Rev.*, **66**, 163–182 (1944).
33. A. Sayah, C. Philipona, P. Lambelet, M. Pfeffer, and F. Marquis-Weible, "Fiber tips for scanning near-field opical microscopy fabricated by normal and reverse etching", *Ultramicroscopy,* **71**, 59–63 (1998).
34. M. Stähelin, M.A. Bopp, G. Tarrach, A.J. Meixner, and I. Zscholle-Gränacher, "Temperature profile of fiber tips used in scanning near-field optical microscopy", *Appl. Phys. Lett.*, **68**, 2603–2605 (1996).
35. D. Zeisel, B. Dutoit, V. Deckert, T. Roth, and R. Zenobi, "Optical spectroscopy and laser desorption on a nanometer scale", *Anal. Chem.*, **69**, 749–754 (1997).
36. E.J. Ayars, H.D. Hallen, and C.L. Jahncke, "Electric field gradient effects in Raman spectroscopy", *Phys. Rev. Lett.*, **85**, 4180–4183 (2000).